



OPEN ACCESS

EDITED BY

Aurea Maria Ciotti,
University of São Paulo, Brazil

REVIEWED BY

Wei Liu,
Shanghai University, China
Montserrat Aldunate,
University of Concepcion, Chile

*CORRESPONDENCE

Alexandra Coello-Camba
✉ acoellocamba@gmail.com

RECEIVED 29 June 2024

ACCEPTED 27 August 2024

PUBLISHED 17 September 2024

CITATION

Coello-Camba A and Agustí S (2024)
Seawater temperature drives the diversity of
key cyanobacteria (*Synechococcus* and
Prochlorococcus) in a warming sea.
Front. Mar. Sci. 11:1456799.
doi: 10.3389/fmars.2024.1456799

COPYRIGHT

© 2024 Coello-Camba and Agustí. This is an
open-access article distributed under the terms
of the [Creative Commons Attribution License
\(CC BY\)](https://creativecommons.org/licenses/by/4.0/). The use, distribution or reproduction
in other forums is permitted, provided the
original author(s) and the copyright owner(s)
are credited and that the original publication
in this journal is cited, in accordance with
accepted academic practice. No use,
distribution or reproduction is permitted
which does not comply with these terms.

Seawater temperature drives the diversity of key cyanobacteria (*Synechococcus* and *Prochlorococcus*) in a warming sea

Alexandra Coello-Camba* and Susana Agustí

Red Sea Research Center, King Abdullah University of Science and Technology (KAUST),
Thuwal, Saudi Arabia

The picocyanobacteria genera *Prochlorococcus* and *Synechococcus* play a significant role globally, dominating the primary production in warm and oligotrophic tropical and subtropical areas, which represent the largest oceanic ecosystem. Genomic studies have revealed high microdiversity within these genera. It is anticipated that ocean warming may cause decreased biodiversity in marine tropical areas, as increasing temperatures may lead to the development of a new thermal niche in these regions. Thus, our study aimed to characterize the microdiversity of picocyanobacteria in the Red Sea, one of the warmest oligotrophic seas on the planet, which is experiencing warming at a rate that exceeds the global average. We identified picocyanobacteria microdiversity in the open waters of the Eastern Red Sea basin, where seawater temperatures ranged from 22.2 to 32.4°C throughout the water column (from surface to 160 m depth). Both *Prochlorococcus* and *Synechococcus* populations were characterized to deep taxonomic levels, applying amplicon sequencing targeting the *petB* gene, revealing up to 15 different (sub)clades. *Synechococcus* dominated the basin, representing an average of 68.8% of the total reads assigned to both cyanobacteria. The subclade *Synechococcus* IIa and *Prochlorococcus* clade HLII were ubiquitous in the water column of the Eastern Red Sea basin, representing 73% and 56% of the *Synechococcus* and *Prochlorococcus* assigned reads, respectively. Maximum cyanobacteria richness was observed at approximately 27.5°C, declining at higher and lower temperatures (polynomial fit, $R^2 = 0.2$, $p < 0.0001$). *Synechococcus* IIa dominated in the warmest surface waters (>30°C) of the Red Sea, displacing other (sub)clades to more saline and nutrient-poor waters, thereby reducing community diversity (polynomial fit, $R^2 = 0.77$, $p < 0.0001$). Our study contributes to identifying changes in picocyanobacterial diversity when exposed to temperatures exceeding current oceanic thermal limits, through the analysis of Red Sea communities already inhabiting such higher-temperature niches.

KEYWORDS

picocyanobacteria, *Prochlorococcus* HLII, *Synechococcus* IIa, microdiversity, warming, Red Sea, temperature

1 Introduction

Oligotrophic areas of the oceans represent >40% of the ocean's surface, and in them, pico-sized phytoplankton is responsible for up to 80%-90% of the primary production (Agawin et al., 2000; Uitz et al., 2010). This extensive surface area is however dominated by two cyanobacterial genera, *Prochlorococcus* and *Synechococcus*, which are described to exhibit high microdiversity within their populations (e.g., Scanlan et al., 2009; Mazard et al., 2012). Different environmental factors shape the microdiversity structure of marine environments, including stratification and mixing processes (Post et al., 2011), nutrient inputs (Spatharis et al., 2007), or salinity (Busseni et al., 2020). Seawater temperature also specifically shapes the diversity of oceanic taxa, which typically peaks in warmer waters (Tittensor et al., 2010; Ibarbalz et al., 2019; Righetti et al., 2019). For cyanobacteria, studies in the Atlantic and Pacific Oceans reported that high seawater temperatures lead to increased *Prochlorococcus* and *Synechococcus* richness indices, respectively (Jameson et al., 2010; Xia et al., 2019). However, in a warming ocean scenario, projected increases in seawater temperatures are expected to alter the composition of phytoplankton communities. Specifically, warming projections are expected to have a detrimental effect on communities inhabiting tropical oceans, where rising temperatures may cause sharp declines in phytoplankton diversities. This reduction in diversity would be caused by the proximity of the thermal optima of tropical phytoplankton taxa to current mean temperatures, and the negative skewness of their thermal tolerance curves, leading to sharp declines in growth rate when subjected to relatively small increases in temperature (Thomas et al., 2012).

Among the world's marine environments, the Red Sea stands out for its characteristically high surface water temperatures, often exceeding 30°C and even surpassing the local historical record of 33°C (Rasul et al., 2015; Chaidez et al., 2017). The main basin is permanently stratified by its strong thermocline, thus limiting the nutrient input from deeper waters toward the oligotrophic shallow waters (Weikert, 1987; Longhurst, 1998). Therefore, this basin is generally considered an oligotrophic system despite a seasonal inflow of nutrient-rich Indian Ocean intermediate water through the Bab-el Mandab Strait at its southernmost limit. In the Red Sea, *Synechococcus* abundances outnumber those of *Prochlorococcus* (Veldhuis and Kraay, 1993; Al-Otaibi et al., 2020; Coello-Camba and Agustí, 2021), thriving in the warm and well-illuminated superficial waters, especially in the southern waters that are characterized by high temperatures (> 30°C) and low salinity (Coello-Camba and Agustí, 2021). In contrast, *Prochlorococcus* thrives in deeper layers mainly towards the Central (Coello-Camba and Agustí, 2021) and North Red Sea (Veldhuis and Kraay, 1993). Previous studies have reported a high abundance of *Synechococcus* clade II and *Prochlorococcus* HLII in the Gulf of Aqaba (Fuller et al., 2003, 2005; Penno et al., 2006; Post et al., 2011), both of which commonly occur in high-temperature and low-nutrient waters (Kent et al., 2018). However, given the steep mean warming rate described for this basin ($0.17 \pm 0.07^\circ\text{C}$ per decade, Chaidez et al., 2017) exceeding the global ocean rate, alterations in the diversity of inhabiting cyanobacterial communities are expected. As part of the tropical ocean, these

key communities in the Red Sea may already be subjected to decreased diversities, therefore compromising the productivity of this ecosystem (Thomas et al., 2012).

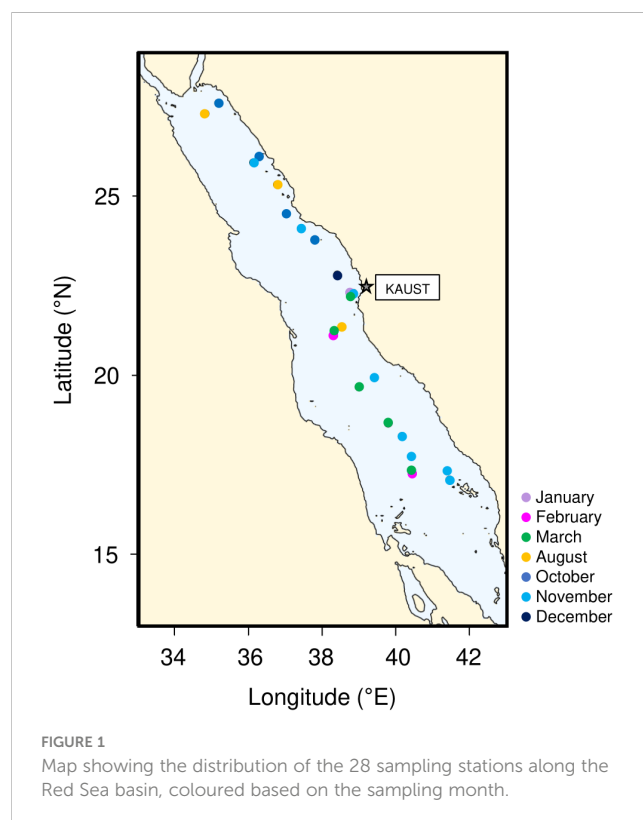
In this study, we characterize the picocyanobacterial communities of the Red Sea by identifying their clade composition, and evaluating various environmental parameters to assess the relationships between clade and subclade distributions and environmental gradients. We calculate cyanobacteria microdiversity indices to examine their variability in response to environmental changes, particularly focusing on Red Sea seawater temperature, which surpasses the maximum surface temperature of tropical oceans by over 2°C. This way, our primary goal is to analyze the temperature-related patterns of picocyanobacterial diversity in one of the warmest marine ecosystems on Earth, where current temperatures closely approximate the projections of thermal niche distributions in the future ocean.

2 Materials and methods

2.1 Sampling

Five different cruises were performed onboard *RV Thuwal* (*Threats*, *Dust*, and *CCF-1* cruises) and *RV Al-Azizi* (*CCF-2* and *3*) from October 2016 to March 2018 (Figure 1; Supplementary Table S1), covering a transect from 17.09 to 27.6°N.

At each station, seawater samples were taken from four depths, distributed from the surface (3-5 m) to a maximum of 160 m, including the deep chlorophyll *a* maximum (DCM). Depending on the vessel, an Idronaut (Ocean Seven 305 Plus) or Sea-Bird (SBE 911



plus)CTD profiler was used to measure the seawater temperature and salinity *in situ*.

Integrated photosynthetically active radiation (PAR, 400–700 nm) and ultraviolet B radiation (UVB, 305 nm) were recorded with a BIC Compact or a PUV-2500 Profiling UV Radiometer (Biospherical Instruments, San Diego, USA), which were deployed at each station at solar noon avoiding shading from the vessel. The diffuse attenuation coefficients (K_d) were estimated as the slopes of the linear regression of the natural logarithm of instantaneous downwelling irradiance ($\mu\text{mol m}^{-2} \text{s}^{-1}$) vs. depth (m).

To measure nutrient concentrations (NO_3 and PO_4), approximately 15-mL seawater samples were kept frozen until analyzed on land using a Segmented Flow Analyzer (SEAL Analytical).

At every sampling location and depth, 300-mL samples were filtered using Whatman GF/F filters to measure chlorophyll *a* (Chl *a*) concentrations, following the fluorometric method described by Parsons et al. (1984). Briefly, 7 mL of 90% acetone was added to the filter and kept refrigerated in the dark for 24 h to extract the pigment. After incubation, we performed sensitive chlorophyll-*a* measurements considering its specific fluorescence excitation and emission wavelengths using a calibrated Trilogy laboratory fluorometer (Turner Designs, Inc.).

To perform cyanobacteria cell counts, we took approximately 1 mL of seawater at each depth. Immediately after sampling, we identified and determined cell abundances using a CyFlow[®] Space flow cytometer equipped with a blue laser beam (488 nm) coupled with a CyFlow[®] autoloading station to facilitate sample loading and processing. The procedures used to analyze these samples are described by Coello-Camba and Agustí (2021).

2.2 DNA extraction, PCR amplification, and sequencing

For DNA analyses, a minimum of 8 L of seawater was obtained from each station and depth. Immediately after sampling, the water samples were filtered through 3 μm and collected on 0.2 μm Isopore[™] membrane filters (142 mm) using a Millipore Masterflex peristaltic pump. The 0.2 μm filters were kept carefully folded in 15 mL plastic tubes and immediately frozen at -80°C .

DNA was extracted using the DNeasy[®] PowerWater[®] DNA Extraction kit (MoBio Laboratories, Inc., Carlsbad, CA). The *petB* gene was selected as a target to assess the microdiversity within *Prochlorococcus* and *Synechococcus* communities, using a *petB* primer set specifically developed and adapted for this purpose (Coello-Camba et al., 2023). PCR amplicons were purified, processed and sequenced by Illumina MiSeq at the KAUST CORELab facilities, following the steps described in Coello-Camba et al. (2023).

2.3 Sequence processing

Raw sequences were processed, analyzed, and filtered using the QIIME 1.9.1 software (Caporaso et al., 2010). Primer sequences

were removed using *cutadapt* (Martin, 2011), and forward and reverse sequences were assembled with PEAR (Zhang et al., 2013) prior to quality filtering. Filtered sequences were then dereplicated with VSEARCH (Rognes et al., 2016), and clustered based on a 94% similarity, as determined by computing within-group distances using Mega 7.0.26 (Tamura et al., 2007). After excluding singletons and chimeras, sequences were classified with MOTHRU (Schloss et al., 2009) against a reference database (Coello-Camba et al., 2023).

2.4 Data analysis

After testing for normal distribution with the D'Agostino-Pearson normality test, we estimated the Spearman correlations between log-transformed environmental data and (sub)clade read proportions using GraphPad Prism[®] 7.0a.

Principal component analysis (PCA) was conducted on log-transformed parameters (except for temperature, salinity, latitude, and depth values) using JMP[®] Pro 12.1.0 to determine the relationships between environmental factors and the distribution of the different *Synechococcus* and *Prochlorococcus* (sub)clades.

Diversity indices, including richness and Shannon index (H'), were calculated for *Synechococcus* and *Prochlorococcus* populations together. The Shannon diversity index was calculated using the `alpha_diversity.py` script in QIIME.

Additionally, a Bray-Curtis distance matrix was calculated as a beta diversity measurement with `vegdist` using the *vegan* package in R (version 3.4.3). Data was previously rarefied to 40,000 sequences per sample and log-transformed. Given that %PAR and %UVB values were not available for all of our samples, these two parameters were excluded from the beta diversity calculations. A multivariate permutational analysis was also conducted to test the significance of the correlation between each environmental variable and the distance matrix with `adonis`. A Mantel test (999 iterations, Spearman correlation) was conducted on the community Bray-Curtis matrix and a Euclidean distance matrix between environmental parameters. Additionally, we selected the Euclidean set of environmental variables that better define the distance matrix using `bioenv`.

The *petB* sequences obtained here from Red Sea samples are deposited at NCBI under BioProject number PRJNA748390.

3 Results

3.1 Cyanobacteria abundance and environmental conditions

During our study along the Red Sea basin, covering a transect of approximately 10 latitudinal degrees (Figure 1), the seawater temperatures averaged (\pm SE) $27.1 \pm 2.6^\circ\text{C}$, varying between 22.2 and 32.4°C and exhibiting a negative correlation with latitude and depth (Supplementary Figure S1; Supplementary Table S2). Salinity ranged from 37.6 to 40.5 psu, with a mean value of 39.4 ± 0.08 psu. Unlike temperature, salinity was positively correlated with latitude

and depth (Supplementary Figure S1; Supplementary Table S2). Moreover, 50% of the incident photosynthetically active radiation (PAR) reached an average (\pm SE) depth of 11.4 ± 2.3 m, whereas 10% and 1% of the PAR reached 38.1 ± 1.7 m depth and 76.7 ± 1.9 m, respectively. For UVB, 50% of the incident radiation reached an average depth of 3.9 ± 2.8 m, whereas 10% of UVB reached 9.2 ± 3.4 m, and 1% UVB reached 16.3 ± 3.2 m (Supplementary Figure S1). Chlorophyll *a* concentration averaged (\pm SE) $0.34 \pm 0.02 \mu\text{g L}^{-1}$, with a maximum of $1.04 \mu\text{g L}^{-1}$ and minimum of $0.01 \mu\text{g L}^{-1}$ (Supplementary Figure S1). Regarding nutrient concentrations, PO_4 and NO_3 mean concentrations (\pm SE) were $0.17 \pm 0.04 \mu\text{M}$ and $1.89 \pm 0.27 \mu\text{M}$, respectively (Supplementary Figure S1).

Picocyanobacteria cell abundances determined via flow cytometry averaged (\pm SE) $1.19 \cdot 10^4 \pm 2.19 \cdot 10^3$ cells mL^{-1} for *Synechococcus* and $7.25 \cdot 10^3 \pm 1.16 \cdot 10^3$ cells mL^{-1} for *Prochlorococcus*. The cell abundance of *Synechococcus* increased towards the south and in surface waters (Supplementary Figure S1; Supplementary Table S2), showing a positive correlation with temperature, %PAR, and %UVB, and a negative correlation with salinity. The correlations between *Prochlorococcus* cell abundance and environmental parameters exhibited opposite trends to those observed for *Synechococcus* but did not vary significantly with latitude (Supplementary Figure S1; Supplementary Table S2). *Synechococcus* and *Prochlorococcus* concentrations were negatively correlated with each other but were positively correlated with chlorophyll *a* concentration (Supplementary Table S2).

3.2 *Synechococcus* and *Prochlorococcus* clades, subclades, and community composition distribution

DNA sequences from 105 samples were processed, and a total of 11,319,755 *petB* reads were obtained; 76.7% of these reads were clustered and assigned to specific *Prochlorococcus* or *Synechococcus* taxa, leaving a total of 456 OTUs classified into (sub)clades. The

proportion of reads assigned to *Prochlorococcus* and *Synechococcus* populations each correlated with the proportion of the respective cell abundances determined with flow cytometry (Spearman's $r=0.33$, Supplementary Figure S2).

We identified a total of 10 clades: 3 *Prochlorococcus* clades (HLI, HLII, and LLI), and 7 *Synechococcus* clades, including CRD1, EnvA, II, III, VII, IX, and WPC1. *Synechococcus* clades II and III were further classified into several subclades (IIa, IIb, IIc, IIE, IIe, IIIa, and IIIb; Figure 2, Supplementary Figure S3). Our analysis also detected the presence of sequences belonging to *Prochlorococcus* or *Synechococcus* genera that could not be further identified and were therefore reported as “unclassified.” However, a BLAST search in the NCBI database (<https://blast.ncbi.nlm.nih.gov/Blast.cgi>) revealed that most of the unclassified *Prochlorococcus* sequences were closely related to low-light adapted branches, with approximately 66% of these reads showing percent identities with LLI clades ranging from 79% to 88%.

The most abundant subclade was *Synechococcus* IIa, with an average proportion (\pm SE) of $62.49 \pm 3.8\%$ of the total reads assigned to both genera (Figure 2). The proportion of subclade IIa showed great variability, from being almost absent in some samples (minimum proportion of 0.04% of total cyanobacteria reads), to dominating the population with more than 99% of the total reads (Figure 2). *Synechococcus* clades CRD1, IX, and IIc exhibited average values of $2.02 \pm 0.96\%$, $4.69 \pm 1.63\%$, and $2.4 \pm 0.39\%$ of total assigned reads respectively (Figure 2), reaching maximum concentrations above 70% for CRD1 and IX, and above 20% for IIc in some samples. The remaining *Synechococcus* groups identified were less represented in the community, with average proportions below 1% of the total cyanobacterial reads. Among these groups, subclade IIIb was the least abundant, being present in only two samples, and was therefore excluded from downstream analyses. The proportion of the most abundant subclade *Synechococcus* IIa decreased with latitude and depth, with negative correlations with salinity and positive correlations with temperature and solar radiation (Table 1; Figure 3). This subclade was positively correlated with Chl *a*

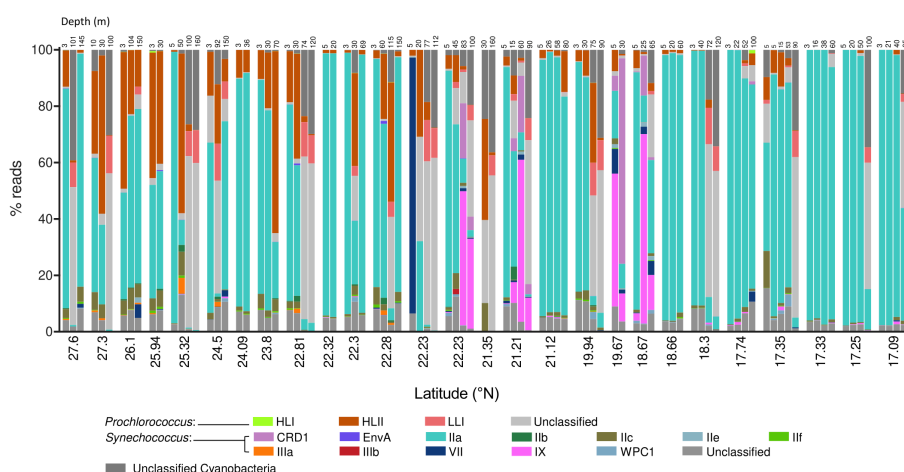


FIGURE 2

Stacked plots of the proportion of reads assigned to *Prochlorococcus* and *Synechococcus* (sub)clades organized by station and depth, from north to south. Samples taken at 22.23°N were taken at the same station during two different cruises and are therefore represented separately.

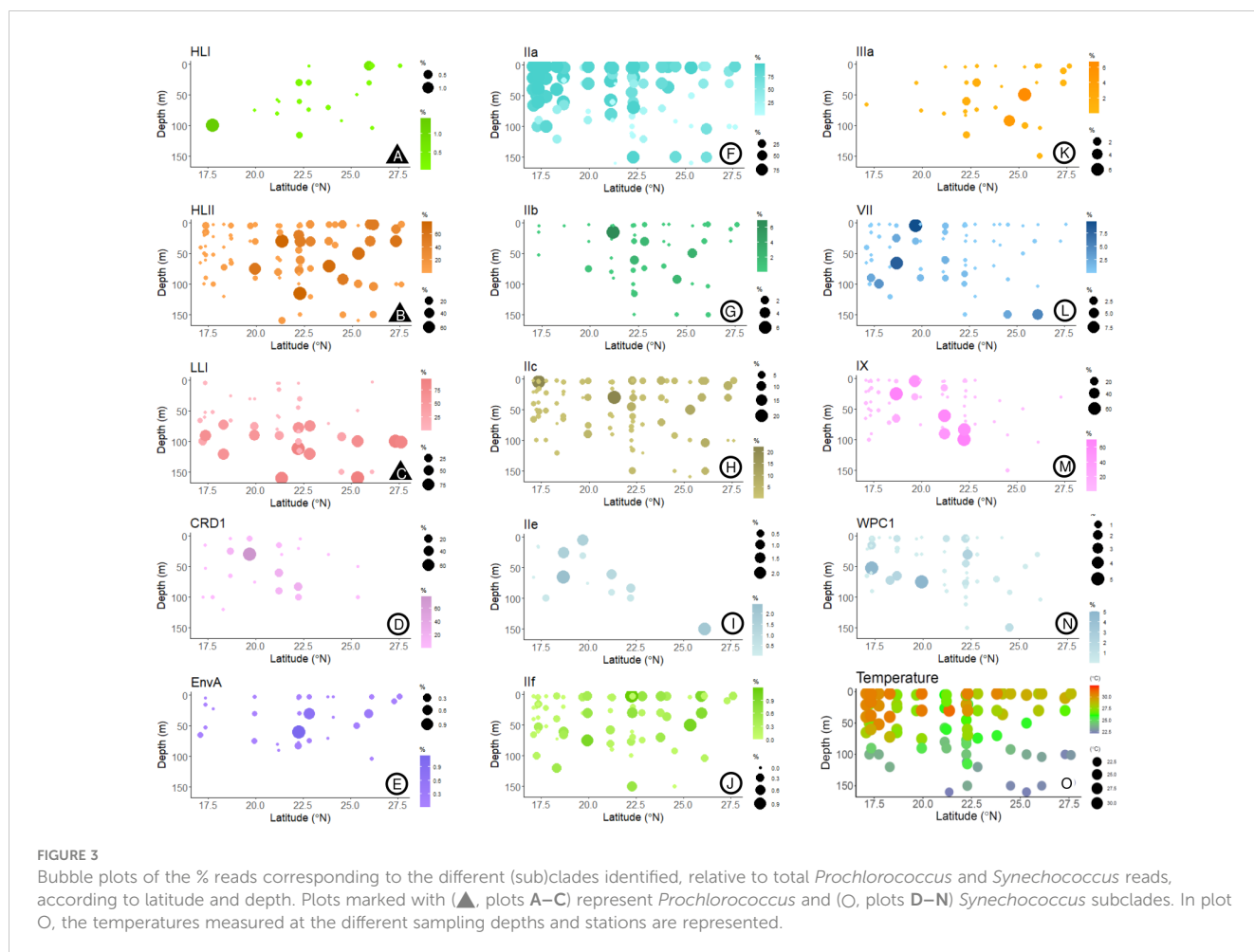
concentration and *Synechococcus* cell abundance and negatively correlated with *Prochlorococcus* cell abundance (Table 1). The proportion of *Synechococcus* IIb reads increased with latitude, salinity, and *Prochlorococcus* cell abundance, and decreased with nutrient concentrations (Table 1; Figure 3). For subclade IIc, the proportions increased with latitude and %UVB and decreased with PO₄ concentration (Table 1; Figure 3). No significant trends were observed for *Synechococcus* IIe (Table 1; Figure 3). For II f, the proportion of reads did not vary with latitude but decreased with depth, being positively correlated with %PAR and %UVB radiation and negatively correlated with PO₄ concentrations (Table 1; Figure 3). The proportion of *Synechococcus* IIIa increased with latitude, salinity, and *Prochlorococcus* cell abundances, and decreased with nutrient concentrations (Table 1; Figure 3). Clade

IX was positively correlated with PO₄ concentration and *Synechococcus* cell abundances but decreased with latitude and salinity (Table 1; Figure 3). Clade VII only showed significant correlations with temperature (negative) and nitrate (positive) (Table 1; Figure 3). *Synechococcus* EnvA exhibited a positive correlation with latitude and a negative correlation with depth and PO₄ concentration (Table 1; Figure 3). For *Synechococcus* CRD1 and WPC1, we did not observe any significant trends associated with the parameters measured herein (Table 1; Figure 3). The samples obtained from 0 to 50 m deep in the southern area (17.09-23.8 °N), where the temperature exceeded 30 °C, were dominated by *Synechococcus* IIa, accounting for an average of 85.6 ± 6% of the total assigned reads. The saltiest waters in the North (≥ 40 psu) were also dominated by this subclade (48.6 ± 5% on average).

TABLE 1 Spearman correlations (p < 0.05) between location, environmental parameters, *Prochlorococcus* and *Synechococcus* cell abundances, and read % for each (sub)clade observed.

| | Assigned read % | | | | | | | | | | | | | |
|-------------------------------|-----------------|-------|-------|-------|-------|-------|-------|-------|------|-------|-------|-------|-------|------|
| | HLI | HLII | LLI | CRD1 | EnvA | IIa | IIb | IIc | Ile | IIf | IIIa | IX | VII | WPC1 |
| Latitude (°N) | 0.40 | 0.59 | ns | ns | 0.28 | -0.46 | 0.53 | 0.30 | ns | ns | 0.51 | -0.47 | ns | ns |
| Depth (m) | ns | ns | 0.65 | ns | -0.21 | -0.51 | ns | ns | ns | -0.23 | ns | ns | ns | ns |
| Temperature (°C) | ns | ns | -0.58 | ns | ns | 0.51 | ns | ns | ns | ns | ns | ns | -0.22 | ns |
| Salinity (psu) | 0.39 | 0.45 | 0.37 | ns | ns | -0.56 | 0.34 | ns | ns | ns | 0.45 | -0.50 | ns | ns |
| % PAR | ns | ns | -0.66 | ns | ns | 0.42 | ns | ns | ns | 0.32 | ns | ns | ns | ns |
| % UVB | ns | ns | -0.62 | ns | ns | 0.33 | ns | 0.26 | ns | 0.35 | ns | ns | ns | ns |
| Chla (µg L ⁻¹) | ns | ns | ns | ns | ns | 0.26 | ns | ns | ns | ns | ns | ns | ns | ns |
| PO ₄ (µM) | -0.39 | -0.46 | 0.33 | ns | -0.43 | ns | -0.51 | -0.27 | ns | -0.30 | -0.50 | 0.23 | ns | ns |
| NO ₃ (µM) | ns | -0.24 | 0.37 | ns | ns | ns | -0.35 | ns | ns | ns | -0.22 | ns | 0.23 | ns |
| Proch. cells mL ⁻¹ | ns | ns | 0.49 | ns | ns | -0.32 | 0.21 | ns | ns | ns | 0.22 | ns | ns | ns |
| Syn. cells mL ⁻¹ | ns | -0.25 | -0.56 | ns | ns | 0.57 | ns | ns | ns | ns | ns | 0.22 | ns | ns |
| Assigned read %: | | | | | | | | | | | | | | |
| HLI | | | | | | | | | | | | | | |
| HLII | 0.58 | | | | | | | | | | | | | |
| LLI | ns | ns | | | | | | | | | | | | |
| CRD1 | ns | ns | ns | | | | | | | | | | | |
| EnvA | 0.45 | 0.39 | ns | ns | | | | | | | | | | |
| IIa | -0.28 | -0.56 | -0.67 | -0.31 | ns | | | | | | | | | |
| IIb | 0.58 | 0.61 | ns | ns | 0.52 | -0.22 | | | | | | | | |
| IIc | 0.41 | 0.54 | ns | ns | 0.45 | ns | 0.34 | | | | | | | |
| Ile | ns | ns | ns | 0.40 | ns | ns | ns | ns | | | | | | |
| IIf | 0.32 | ns | ns | ns | 0.54 | ns | 0.42 | 0.53 | ns | | | | | |
| IIIa | 0.65 | 0.61 | ns | ns | 0.50 | -0.36 | 0.68 | 0.41 | ns | 0.26 | | | | |
| IX | ns | -0.33 | ns | 0.36 | ns | ns | ns | ns | 0.37 | ns | ns | | | |
| VII | ns | ns | ns | 0.35 | ns | ns | ns | ns | 0.41 | ns | ns | 0.43 | | |
| WPC1 | ns | ns | ns | ns | 0.27 | ns | 0.26 | ns | 0.21 | 0.34 | ns | 0.45 | 0.31 | |

Non-significant correlations are marked with ns.



For *Prochlorococcus*, clades HLII and LLI accounted for $13.6 \pm 2.1\%$ and $12.8 \pm 2.8\%$ (Mean \pm SE) of total reads assigned to both genera, respectively, with clade HLII presented in all but one of the samples examined. Whereas HLI was the least abundant *Prochlorococcus* group with a mean of $0.04 \pm 0.02\%$ of total assigned reads (Figure 2). The proportions of total reads assigned to *Prochlorococcus* HLI and HLII increased significantly with latitude but were largely unaffected by depth (Table 1; Figure 3). Further, the proportions of both groups increased with salinity and decreased with PO_4 concentrations, and HLII also decreased with NO_3 concentrations (Table 1). Interestingly, the proportion of reads assigned to *Prochlorococcus* LLI did not vary with latitude, but increased with depth, salinity, and nutrients, and decreased with temperature and both %PAR and %UVB radiations (Table 1; Figure 3). Both HLII and LLI were negatively correlated with *Synechococcus* cell concentrations, and LLI correlated positively with *Prochlorococcus* cell concentrations (Table 1).

Prochlorococcus HLI, HLII, and *Synechococcus* EnvA, Iib, Iic, IIf, and IIIa correlated positively with each other (except IIf with HLII) (Table 1). *Prochlorococcus* LLI only exhibited a single significant negative correlation with *Synechococcus* Iia (Table 1). The proportion of the abundant *Synechococcus* Iia was negatively correlated with the three identified *Prochlorococcus* groups and with *Synechococcus* CRD1, Iib, and IIIa (Table 1). *Synechococcus* CRD1,

Iie, IX, and VII correlated positively with each other, and clade IX also correlated negatively with HLII (Table 2). *Synechococcus* WPC1 correlated positively with EnvA, Iib, Iie, IIf, IX, and VII (Table 1).

A principal component analysis (PCA) elucidated strong correlations between depth, %PAR, temperature, salinity, %UVB, and NO_3 concentration on the proportion of reads assigned to *Prochlorococcus* LLI and *Synechococcus* Iia (Figure 4; Table 2). The proportion of *Prochlorococcus* LLI reads increased significantly in samples collected from deeper, colder, and less illuminated waters under higher salinity and nitrate concentrations, whereas *Synechococcus* Iia exhibited the opposite response to these factors (Figure 4; Table 2). Furthermore, cell concentrations were also significantly correlated with the proportion of reads of both groups, with LLI being positively correlated with *Prochlorococcus* cell abundance and negatively correlated with *Synechococcus* cell abundance. For *Synechococcus* Iia, the correlations with cell abundances exhibited the opposite trend (Figure 4; Table 2). Latitude and salinity affected most of the read proportions assigned to other groups, with both parameters exhibiting a positive correlation with *Prochlorococcus* HLII and *Synechococcus* EnvA, Iib, Iic, IIf, and IIIa, and a negative correlation with *Synechococcus* CRD1, Iie, and IX (Figure 4; Table 2). Nutrient concentrations had a less pronounced effect on clade relative abundances than latitude and salinity, albeit with an opposite sign (Figure 4; Table 2). Further, we

TABLE 2 Loading values for each component of the PCA plot in Figure 4.

| | | PC1 | PC2 |
|---|-----------------|-------|-------|
| Log _{10%} reads | HLI | 0.11 | 0.15 |
| | HLII | 0.11 | 0.76 |
| | LLI | 0.75 | -0.03 |
| | CRD1 | 0.23 | -0.50 |
| | EnvA | 0.01 | 0.46 |
| | Ila | -0.65 | -0.07 |
| | Ilb | 0.13 | 0.56 |
| | Ilc | -0.10 | 0.57 |
| | Ile | 0.28 | -0.45 |
| | Ilf | -0.13 | 0.47 |
| | IIIa | 0.19 | 0.63 |
| | IX | 0.20 | -0.57 |
| | VII | 0.35 | -0.42 |
| | WPC1 | 0.08 | 0.04 |
| Latitude (°N) | Latitude | 0.34 | 0.67 |
| Depth (m) | Depth | 0.92 | -0.02 |
| Temp. (°C) | Temp. | -0.85 | -0.04 |
| Salinity (psu) | Salinity | 0.62 | 0.56 |
| Log _{10%} PAR | %PAR | -0.90 | 0.16 |
| Log _{10%} UVB | %UVB | -0.65 | 0.15 |
| Log ₁₀ µg Chla L ⁻¹ | Chla | -0.22 | -0.04 |
| Log ₁₀ µM PO ₄ | PO ₄ | 0.12 | -0.35 |
| Log ₁₀ µM NO ₃ | NO ₃ | 0.51 | -0.34 |
| Log ₁₀ <i>Prochlorococcus</i> mL ⁻¹ | Pro. | 0.49 | 0.15 |
| Log ₁₀ <i>Synechococcus</i> mL ⁻¹ | Syn. | -0.72 | -0.11 |

did not identify clear trends for *Prochlorococcus* HLI and *Synechococcus* VII and WPC1 read proportions (Figure 4; Table 2).

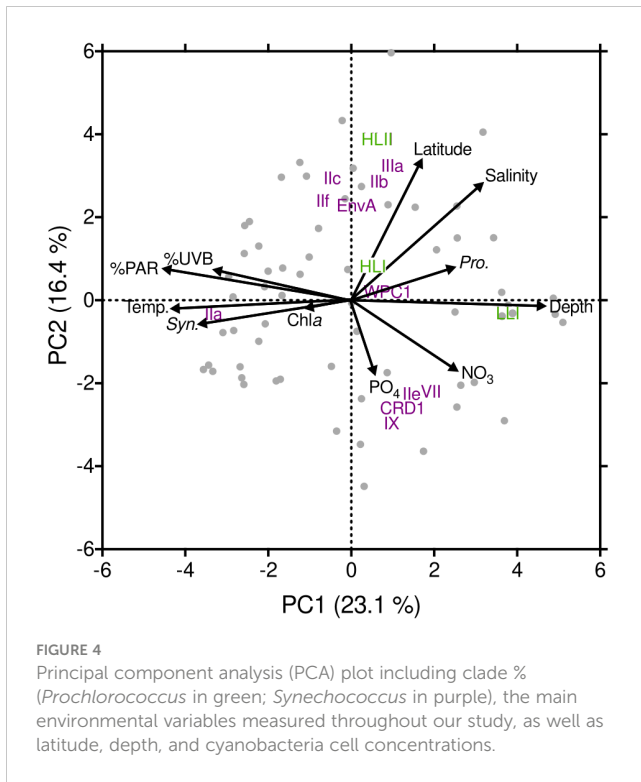
3.3 Diversity indices

The (sub)clade richness and Shannon index for each sample were determined as indicators of alpha diversity. The average (\pm SE) (sub)clade richness estimated from our samples was 9 ± 0.3 (sub)clades per sample. The lowest richness value was observed in a sample taken at 160 m depth, in a central Red Sea station, where only 3 groups were identified, including *Prochlorococcus* HLI and HLII and a small proportion of *Synechococcus* Ila. The maximum richness value was 14, also observed in the DCM of the central Red Sea where all the *Prochlorococcus* and *Synechococcus* (sub)clades identified in this study were observed. Cyanobacteria richness

reached a maximum value at 27.1°C (polynomial fit, $R^2 = 0.2$, $p < 0.0001$, Figure 5 plot A); the richness of *Synechococcus* clades alone reached a maximum value at a similar temperature (27.3°C), whereas no significant trends were found when considering only *Prochlorococcus*. Richness did not show any significant correlation with salinity but did exhibit significant, albeit weak, negative relationships with phosphate ($p = 0.006$) and nitrate ($p = 0.04$). With regards to cell abundances, we observed a maximum richness value at *Synechococcus* concentrations of approximately 2300 cells mL⁻¹ (polynomial fit, $R^2 = 0.32$, $p < 0.0001$, Figure 5 plot B). Richness decreased linearly with increasing LLI proportion in the samples (slope = -0.04, $p < 0.0001$) and increased significantly with the proportions of EnvA (slope = 4.04, $p = 0.01$), IIf (slope = 3.77, $p < 0.0001$), WPC1 (slope = 0.89, $p = 0.001$), and IIIa (slope = 0.64, $p = 0.02$).

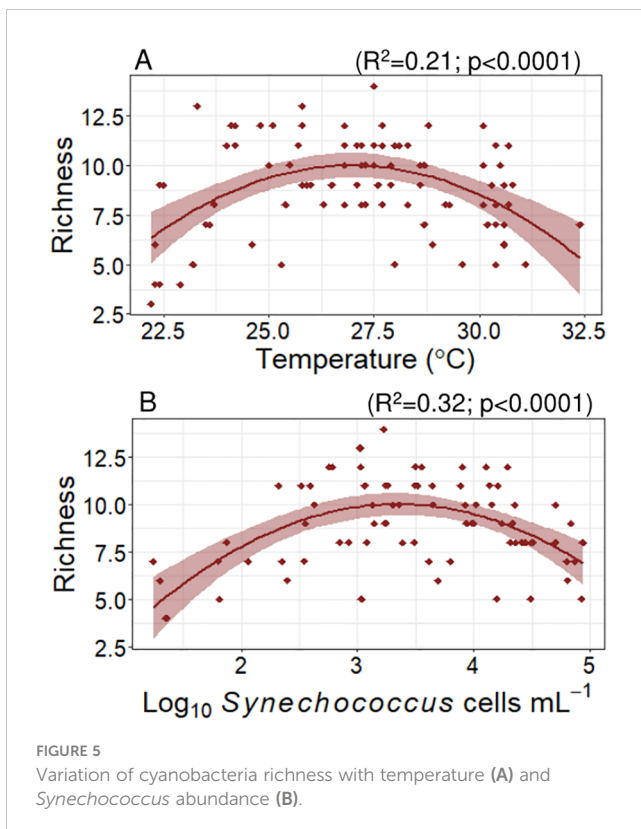
Shannon's index averaged 0.58 ± 0.04 and varied between 0.02 and 1.43. This diversity index reached maximum values with latitude at 24.2°N (polynomial fit, $R^2 = 0.12$, $p = 0.001$). The Shannon index increased linearly with salinity (slope = 0.2 ± 0.05 , $R^2 = 0.13$, $p = 0.0002$) and did not show any significant correlation with nutrients concentrations. This index showed a polynomial relationship with *Synechococcus* abundance, showing maximum values at *Synechococcus* concentrations close to 600 cells mL⁻¹ (polynomial fit, $R^2 = 0.46$, $p < 0.0001$, Figure 6 plot A). Considering the proportion of *Synechococcus* Ila in the samples, the Shannon index reached its maximum at a 40% *Synechococcus* Ila proportion (polynomial fit, $R^2 = 0.77$, $p < 0.0001$, Figure 6 plot B), showing a sharp decrease at lower and higher proportions. For *Prochlorococcus* clades, the maximum Shannon indices were observed at proportions of 45% *Prochlorococcus* HLII ($R^2 = 0.35$, $p = 0.0001$, Figure 6 plot C) and 42% LLI ($R^2 = 0.22$, $p = 0.0001$). We did not observe any significant correlations between the Shannon index and other detected (sub)clades.

Next, a Bray-Curtis dissimilarity matrix was calculated to determine the inter-sample diversity (beta diversity). The results of the Mantel test confirmed that there was a significant relationship between the dissimilarity and the Euclidean environmental matrices ($r = 0.34$, $p = 0.001$), indicating that the changes in cyanobacterial community composition were modulated by the environment. According to the results of our bioenv test, the set of environmental variables that best explained the dissimilarity matrix were temperature, salinity, and nitrate concentrations ($r = 0.36$). Adonis analyses were then conducted to test which individual variables correlated best with the changes in community assemblages observed herein. Our results indicated that depth (explaining 19.1% of the variation), temperature (15.4%), salinity (15.0%), latitude (11.8%), and *Synechococcus* cell abundances (11%) had the strongest effect on the lineage composition between samples, followed by nutrients (PO₄: 4.8%, NO₃: 7.5%) and *Prochlorococcus* abundances (6.6%). Further, using a pairwise adonis function, we identified significant differences between the beta-diversities of samples obtained from the southern basin ($< 19^\circ$ N) and samples from the rest of the basin (F Model = 10.28, $R^2 = 0.11$, $p = 0.001$).



4 Discussion

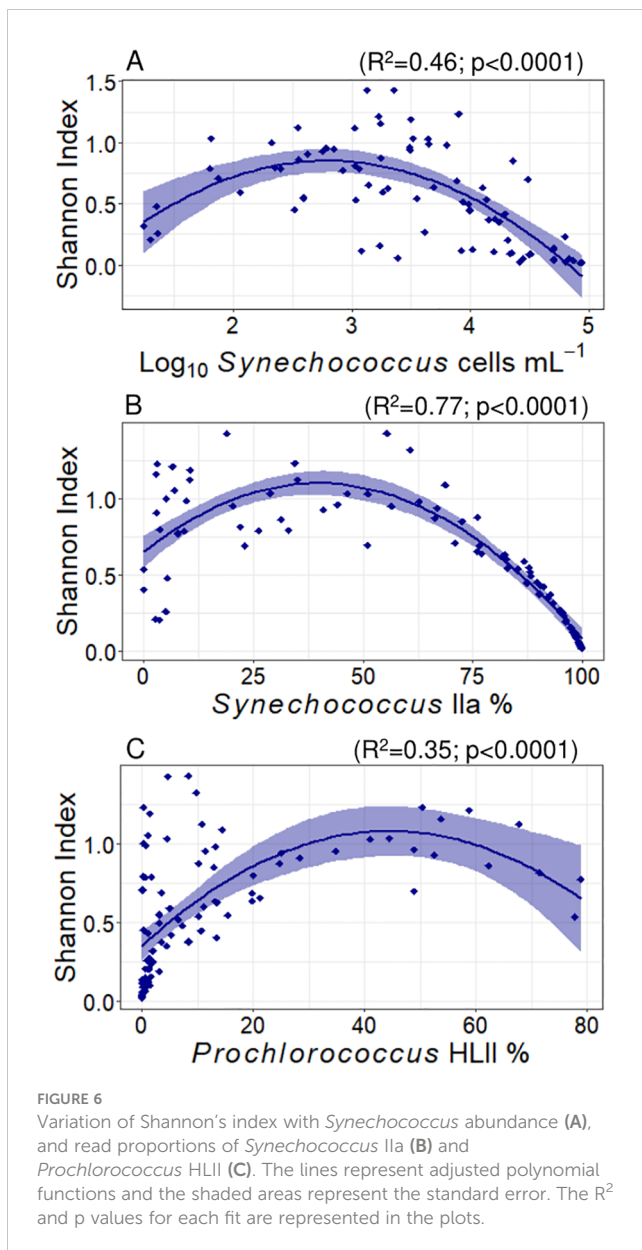
Our genetic analyses of Red Sea samples elucidated the presence of up to 15 different *Synechococcus* and *Prochlorococcus* (sub)clades,



with a predominance of *Prochlorococcus* HLII and *Synechococcus* subclade Ila, ubiquitous in the photic layer of the Eastern basin, both typical of high-temperature, low-macronutrient, and iron-sufficient waters (Kent et al., 2018). Our findings indicated that clade distribution was strongly influenced by environmental gradients in the Red Sea basin, picocyanobacterial richness showing a bimodal distribution with temperature, showing maximum at 27.3°C, decreasing at lower and higher temperatures. The warmest waters ($\geq 30^\circ\text{C}$) were dominated by *Synechococcus* Ila, the most abundant group in the entire basin, and its increasing dominance resulted in a notable decrease in community diversity. For the deepest samples analyzed, we observed an increase in unclassified *Prochlorococcus* reads below the DCM layer, as observed by Shibl et al. (2016).

We assigned *Prochlorococcus* reads to 3 different clades, similar to the clade richness obtained targeting the internal transcribed spacer region (ITS) in surface waters of the North Pacific (Choi et al., 2011, 2013; Larkin et al., 2016), but less than those found in other oligotrophic areas (Huang et al., 2012; Shibl et al., 2014; Affe et al., 2018). In the Red Sea, Shibl et al. (2014) identified up to 8 different *Prochlorococcus* clades, mostly dominated by HLII. *Prochlorococcus* HLII was ubiquitous and the most abundant *Prochlorococcus* clade found in our study, which was also consistent with previous studies in the region (West et al., 2001; Fuller et al., 2005; Penno et al., 2006; Ngugi et al., 2012; Shibl et al., 2014; 2016). We found lower abundances of *Prochlorococcus* HLI, and LLI, as observed for the Gulf of Aqaba in the Northern Red Sea (West et al., 2001; Fuller et al., 2005). *Prochlorococcus* clades were distributed down the water column following a vertical partition, where *Prochlorococcus* HLII dominated closer to the surface and was present along the water column. A similar result was reported by Shibl et al. (2014) for the Red Sea, highlighting the predominance of HLII even below 200 m deep. *Prochlorococcus* LLI showed increased proportions below 70 m depths, where PAR was approximately $< 1\%$, matching the niche distribution of *Prochlorococcus* cell abundances in the Red Sea, characterized by low illuminated and colder waters under higher salinities and nutrient concentrations (Coello-Camba and Agustí, 2021). Seawater temperature (Martiny et al., 2006, 2009) and salinity (Larkin et al., 2016) have been defined as important determinants of the relative abundance of *Prochlorococcus* HL ecotypes in oceans. *Prochlorococcus* HLII exhibited a positive correlation with increasing latitude and salinity, with HLI being absent from the southernmost and more superficial samples. The shift from clade HLII to clade HLI towards higher latitudes and colder waters observed here was consistent with the similar distribution of these clades reported elsewhere (Johnson et al., 2006; Zwirgmaier et al., 2008; Huang et al., 2012).

There are few studies documenting the clades composition of *Synechococcus* in the Red Sea. In our investigation, we determined the presence of 7 *Synechococcus* clades, in line with the 8 and 10 *Synechococcus* clades identified by Post et al. (2011) and Fuller et al. (2003), respectively, in the Gulf of Aqaba (Northern Red Sea). We observed that *Synechococcus* clade II was both ubiquitous and predominant across the Eastern Red Sea basin. Notably, our study encompassed a broader geographical area and water column than



previous research on both *Prochlorococcus* and *Synechococcus* populations of the Red Sea, further reinforcing the overwhelming dominance of *Synechococcus* clade II in these waters. Clade II was also found to thrive in surface waters of the Indian Ocean (Farrant et al., 2016) and tropical and subtropical areas of the Pacific gyres (Xia et al., 2019), the California Current (Toledo and Palenik, 2003), and the northern part of the Arabian Sea (Fuller et al., 2006). Zwirgmaier et al. (2008) demonstrated that this clade was associated with warm waters ranging from 22°C to 28°C in the Moroccan Atlantic, whereas other clades either possessed a wider temperature tolerance range or were restricted to cooler waters. In addition to this clade, we identified several *Synechococcus* clades, including clades III, VII, and IX, which had been previously detected in the Gulf of Aqaba in the northern Red Sea (Fuller et al., 2003, 2005; Penno et al., 2006). We also identified the presence of clades WPC1, EnvA, and CRD1 in the Red Sea,

described elsewhere (Saito et al., 2005; Choi and Noh, 2009; Mazard et al., 2012).

The distribution of the predominant *Synechococcus* IIa exhibited a positive correlation with both %PAR and %UVB, significantly increasing in warmer, well-illuminated waters characterized by low salinity and nitrate concentrations. However, this subclade was particularly favored by the warmest conditions (>30°C), being temperature the primary factor influencing its abundance in our study, while other *Synechococcus* II subclades showed minimal response. In the Eastern Red Sea basin, picophytoplankton populations are strongly influenced by temperature, which stands out as the predominant environmental factor shaping their distribution (Coello-Camba and Agustí, 2021). Furthermore, the distribution of cyanobacteria is influenced by competitive interactions among different populations, which play a significant role in defining and partitioning their realized niches. The realized niche of *Synechococcus* in the Red Sea is centered around 30°C, with this cyanobacterium dominating the picophytoplankton community in warmer waters (Coello-Camba and Agustí, 2021). Specifically, our results indicate that these warmer waters are predominantly inhabited by subclade IIa.

Temperature affects metabolic processes, with higher temperatures increasing the rate of metabolic reactions and therefore controlling ecological processes at all levels of organization (Brown et al., 2004). Temperature has also been defined as a fundamental factor that enhances the diversity of marine taxa in general (Tittensor et al., 2010), and phytoplankton groups in particular (Ibarbalz et al., 2019; Righetti et al., 2019; Busseni et al., 2020) explaining more than two-thirds of the global variations in phytoplankton richness (Righetti et al., 2019). Cyanobacterial richness increased with increasing temperature as is described in global models but the high temperatures that characterize the Red Sea (Chaidez et al., 2017) have gradually decreased the richness of the native cyanobacterial communities, and have led to the overwhelming predominance of *Synechococcus* subclade IIa. These temperatures exceed the highest ocean temperatures reported in global phytoplankton diversity studies by >1.5–2°C (Ibarbalz et al., 2019; Righetti et al., 2019) and may be characteristic of the predicted new “thermal niches” that may experience tropical species with ocean warming (Thomas et al., 2012).

It has been hypothesized that bacterial communities consist of a core community of abundant groups that are responsible for most biogeochemical functions (e.g., carbon fixing or nitrogen cycling) and a group of rare members that provide a background of genomic potential (Höfle et al., 2008; Galand et al., 2009; Pedrós-Alió, 2012). Based on the arbitrary relative abundance cut-off value of 1% that is widely used to discriminate between abundant and rare groups (Galand et al., 2009; Pedrós-Alió, 2012; Vergin et al., 2013), only 6 of the (sub)clades detected in our study can be considered abundant, including *Prochlorococcus* HLII, LLI, and *Synechococcus* IIa, IIC, IX, and CRD1. Among the less abundant (sub)clades identified herein, we observed a significant contribution of *Synechococcus* EnvA, IIF, IIIa, and WPC1 to the richness values. The rare members of a microbial community contribute

significantly to its richness and biodiversity (Pedrós-Alió, 2012; Lynch and Neufeld, 2015), maintaining the balance and function of ecosystems by enhancing the metabolic and genetic potential of the community (e.g., Jousset et al., 2017). These groups may also play a role as a “seed bank,” offering a pool of genetic resources that may act as a “safety net” for the community under changing conditions (Vergin et al., 2013; Jousset et al., 2017). Our results indicated that the relative proportions of the rare groups sporadically surpassed the 1% cut-off value, but never in samples taken at temperatures above 30°C, where *Synechococcus* IIa is overwhelmingly predominant and displaces *Prochlorococcus* and less abundant subclades from the community. We also observed a slowdown in the increasing trend of cyanobacterial diversity at the warmest range of the tested temperatures, reaching a maximum richness value at 27.1°C, and decreasing at higher temperatures, as *Synechococcus* IIa becomes overwhelmingly predominant and reaches average proportions of 86.5% at temperatures above 30°C.

Overall, the range of Shannon indices (0.02–1.43) observed in our study matched the values observed in picocyanobacteria communities from different sites. Choi et al. (2011) reported low Shannon indices (averaging approximately 0.08) in surface cyanobacterial populations that inhabited warm (29–30.9°C) oligotrophic open ocean stations in the tropical Pacific Ocean and were dominated by *Prochlorococcus* HLII. However, as conditions changed towards colder and more nutrient-rich coasts, *Synechococcus* populations grew and diversified, leading to peaks in Shannon indices (up to approximately 1.8). The decreased Shannon index observed in our study reflects the *Synechococcus* IIa increased predominance in the population, thus leading to an overall decrease in (sub)clade diversity as well as to lower equity in the relative abundances of the (sub)clades represented.

We observed a positive correlation between salinity and Shannon diversity, also detected for *Synechococcus* populations in coastal waters near Hong Kong (Xia et al., 2017). In contrast, nutrient concentrations did not affect the alpha diversity values. Previous observations indicate that nutrient inputs can have different effects on the diversity of phytoplankton communities, either by stimulating the growth of several groups or decreasing diversity due to the dominance of a single blooming species (Spatharis et al., 2007). A previous mesocosm experiment in Red Sea waters determined that the *Synechococcus* community diversity did not vary during a bloom triggered by nutrient inputs, where, in agreement with our results, clade IIa dominated the community before and immediately after the event, before being decimated by virus infection (Coello-Camba et al., 2020).

Temperature has been defined as a relevant factor in explaining and predicting the global patterns of species richness across major marine groups, ranging from zooplankton to marine mammals (Tittensor et al., 2010). Surface seawater temperature (SST) was found to be the only statistically significant predictor (including primary productivity, oxygen stress and temporal stability) explaining diversity (Tittensor et al., 2010), supporting the kinetic energy hypothesis, which implies that higher metabolic rates or relaxed thermal constraints promote diversity. For phytoplankton groups in particular, Ibarbalz et al. (2019) found that SST was strongly and positively associated with diversity patterns of marine

plankton groups across the oceans, explaining overall more than two-thirds of the global variations in phytoplankton richness (Righetti et al., 2019). In a transect through the North Pacific, Xia et al. (2019) observed an increase in the species richness of surface *Synechococcus* assemblages in response to water temperature, which coincided with a shift in the predominant clade from *Synechococcus* I in the coldest waters to clade CRD1 in the warmest areas. This is particularly noticeable in the warmest areas where *Synechococcus* reaches its highest abundance (Coello-Camba and Agustí, 2021). Different studies highlighted the relevance of temperature in driving marine diversity, suggesting that changes in the temperature of the ocean due to warming may have strong consequences for the distribution of marine biodiversity (Ibarbalz et al., 2019; Busseni et al., 2020), including picocyanobacterial taxa, as found in our study.

Therefore, our findings provide important insights into the major environmental factors that shape the diversity of cyanobacterial communities in the Red Sea, as well as the preponderant influence of temperature on (sub)clade distributions and dominance. The highest temperatures led to decreased population diversity as *Synechococcus* IIa thrived at the expense of displacing other (sub)clades. Using the Red Sea as a gauge for the future global ocean, we could therefore expect thriving *Synechococcus* populations with decreased microdiversity, posing a potential threat to the metabolic and genetic capabilities of the planktonic community in a high-temperature scenario.

Data availability statement

The datasets presented in this study can be found in online repositories. The names of the repository/repositories and accession number(s) can be found below: <https://www.ncbi.nlm.nih.gov/>, PRJNA748390.

Author contributions

AC-C: Formal analysis, Investigation, Writing – original draft, Writing – review & editing. SA: Conceptualization, Investigation, Writing – original draft, Writing – review & editing.

Funding

The author(s) declare financial support was received for the research, authorship, and/or publication of this article. This research was supported by King Abdullah University of Science and Technology through baseline funding BAS/1/1072-01-01 to SA and FCC/1/1973-21-01.

Acknowledgments

We thank the technical personnel of the Coastal and Marine Resources Core Laboratory (CMOR) and the RV Thuwal and RV

Al-Azizi crews for their assistance during sampling. We also thank Dr. R. Díaz-Rúa for his invaluable contributions to our primer design, DNA extraction, and sequencing procedures.

Conflict of interest

The authors declare that the research was conducted in the absence of any commercial or financial relationships that could be construed as a potential conflict of interest.

The author(s) declared that they were an editorial board member of Frontiers, at the time of submission. This had no impact on the peer review process and the final decision.

References

- Affe, H. M. J., Rigonato, J., Nunes, J. M. C., and Menezes, M. (2018). Metagenomic analysis of cyanobacteria in an oligotrophic tropical estuary, South Atlantic. *Front. Microbiol.* 9. doi: 10.3389/fmicb.2018.01393
- Agawin, N. S., Duarte, C. M., and Agustí, S. (2000). Nutrient and temperature control of the contribution of picoplankton to phytoplankton biomass and production. *Limnol. Oceanogr.* 45, 591–600. doi: 10.4319/lo.2000.45.3.0591
- Al-Otaibi, N., Huete-Staufer, T. M., Calleja, M., Irigoien, X., and Morán, X. A. G. (2020). Seasonal variability and vertical distribution of autotrophic and heterotrophic picoplankton in the Central Red Sea. *PeerJ* 8, e8612. doi: 10.7717/peerj.8612
- Brown, J. H., Gillooly, J. F., Allen, A. P., Savage, V. M., and West, G. B. (2004). Toward a metabolic theory of ecology. *Ecology* 85, 1771–1789. doi: 10.1890/03-9000
- Busseni, G., Caputi, L., Piredda, R., Fremont, P., Mele, B. H., Campese, L., et al. (2020). Large scale patterns of marine diatom richness: Drivers and trends in a changing ocean. *Global Ecol. Biogeogr.* 00, 1–14. doi: 10.1111/geb.13161
- Caporaso, J. G., Kuczynski, J., Stombaugh, J., Bittinger, K., Bushman, F. D., Costello, E. K., et al. (2010). QIIME allows analysis of high-throughput community sequencing data. *Nat. Methods* 7, 335. doi: 10.1038/nmeth.f303
- Chaidez, V., Dreano, D., Agustí, S., Duarte, C. M., and Hoteit, I. (2017). Decadal trends in Red Sea maximum surface temperature. *Sci. Rep.* 7, 1–8. doi: 10.1038/s41598-017-08146-z
- Choi, D. H., and Noh, J. H. (2009). Phylogenetic diversity of *Synechococcus* strains isolated from the East China Sea and the East Sea. *FEMS Microbiol. Ecol.* 69, 439–448. doi: 10.1111/j.1574-6941.2009.00729.x
- Choi, D. H., Noh, J. H., Hahn, M. S., and Lee, C. M. (2011). Picocyanobacterial abundances and diversity in surface water of the northwestern Pacific Ocean. *Ocean. Sci. J.* 46, 265–271. doi: 10.1007/s12601-011-0020-0
- Choi, D. H., Noh, J. H., and Shim, J. S. (2013). Seasonal changes in picocyanobacterial diversity as revealed by pyrosequencing in temperate waters of the East China Sea and the East Sea. *Aquat. Microb. Ecol.* 7, 75–90. doi: 10.3354/ame01669
- Coello-Camba, A., and Agustí, S. (2021). Picophytoplankton niche partitioning in the warmest oligotrophic sea. *Front. Mar. Sci.* 8. doi: 10.3389/fmars.2021.651877
- Coello-Camba, A., Diaz-Rua, R., Duarte, C. M., Irigoien, X., Pearman, J. K., Alam, I., et al. (2020). Picocyanobacteria community and cyanophage infection responses to nutrient enrichment in a mesocosms experiment in oligotrophic waters. *Front. Microbiol.* 11. doi: 10.3389/fmicb.2020.01153
- Coello-Camba, A., Diaz-Rua, R., and Agustí, S. (2023). Design and use of a new primer pair for the characterization of the cyanobacteria *Synechococcus* and *Prochlorococcus* communities targeting petB gene through metabarcoding approaches. *MethodsX* 11, 102444. doi: 10.1016/j.mex.2023.102444
- Farrant, G. K., Doré, H., Cornejo-Castillo, F. M., Partensky, F., Ratin, M., Ostrowski, M., et al. (2016). Delineating ecologically significant taxonomic units from global patterns of marine picocyanobacteria. *P. Nat. A. Sci.* 113, E3365–E3374. doi: 10.1073/pnas.1524865113
- Fuller, N. J., Marie, D., Partensky, F., Vaulot, D., Post, A. F., and Scanlan, D. J. (2003). Clade-specific 16S ribosomal DNA oligonucleotides reveal the predominance of a single marine *Synechococcus* clade throughout a stratified water column in the Red Sea. *Appl. Environ. Microbiol.* 69, 2430–2443. doi: 10.1128/AEM.69.5.2430-2443.2003
- Fuller, N. J., Tarran, G. A., Yallop, M., Orcutt, K. M., and Scanlan, D. J. (2006). Molecular analysis of picocyanobacterial community structure along an Arabian Sea transect reveals distinct spatial separation of lineages. *Limnol. Oceanogr.* 51, 2515–2526. doi: 10.4319/lo.2006.51.6.2515
- Fuller, N. J., West, N. J., Marie, D., Yallop, M., Rivlin, T., Post, A. F., et al. (2005). Dynamics of community structure and phosphate status of picocyanobacterial populations in the Gulf of Aqaba, Red Sea. *Limnol. Oceanogr.* 50, 363–375. doi: 10.4319/lo.2005.50.1.0363
- Galand, P. E., Casamayor, E. O., Kirchman, D. L., and Lovejoy, C. (2009). Ecology of the rare microbial biosphere of the Arctic Ocean. *P. Nat. A. Sci.* 106, 22427–22432. doi: 10.1073/pnas.0908284106
- Höfle, M. G., Kirchman, D., Christen, R., and Brettar, I. (2008). Molecular diversity of bacterioplankton: link to a predictive biogeochemistry of pelagic ecosystems. *Aquat. Microb. Ecol.* 53, 39–58. doi: 10.3354/ame01227
- Huang, S., Wilhelm, S. W., Harvey, H. R., Taylor, K., Jiao, N., and Chen, F. (2012). Novel lineages of *Prochlorococcus* and *Synechococcus* in the global oceans. *ISME J.* 6, 285–297. doi: 10.1038/ismej.2011.106
- Ibarbalz, F. M., Henry, N., Brandaño, M. C., Martini, S., Busseni, G., Byrne, H., et al. (2019). Global trends in marine plankton diversity across kingdoms of life. *Cell* 179, 1084–1097. doi: 10.1016/j.cell.2019.10.008
- Jameson, E., Joint, I., Mann, N. H., and Mühling, M. (2010). Detailed analysis of the microdiversity of *Prochlorococcus* populations along a North-South Atlantic Ocean transect. *Environ. Microbiol.* 12, 156–171. doi: 10.1111/j.1462-2920.2009.02057.x
- Johnson, Z. I., Zinser, E. R., Coe, A., McNulty, N. P., Woodward, E. M. S., and Chisholm, S. W. (2006). Niche partitioning among *Prochlorococcus* ecotypes along ocean-scale environmental gradients. *Science* 311, 1737–1740. doi: 10.1126/science.1118052
- Joussot, A., Bienhold, C., Chatzinotas, A., Gallien, L., Gobet, A., Kurm, V., et al. (2017). Where less may be more: how the rare biosphere pulls ecosystems strings. *ISME J.* 11, 853–862. doi: 10.1038/ismej.2016.174
- Kent, A. G., Baer, S. E., Mougnot, C., Huang, J. S., Larkin, A. A., Lomas, M. W., et al. (2018). Parallel phylogeography of *prochlorococcus* and *synechococcus*. *ISME J.* 13, 430–441. doi: 10.1038/s41396-018-0287-6
- Larkin, A. A., Blinbry, S. K., Howes, C., Lin, Y., Loftus, S. E., Schmaus, C. A., et al. (2016). Niche partitioning and biogeography of high light adapted *Prochlorococcus* across taxonomic ranks in the North Pacific. *ISME J.* 10, 1555–1567. doi: 10.1038/ismej.2015.244
- Longhurst, A. R. (1998). *Ecological Geography of the Sea* (Michigan: Academic Press).
- Lynch, M. D. J., and Neufeld, J. D. (2015). Ecology and exploration of the rare biosphere. *Nat. Rev.: Microbiol.* 13, 217–229. doi: 10.1038/nrmicro3400
- Martín, M. (2011). Cutadapt removes adapter sequences from high-throughput sequencing reads. *EMBnet. J.* 17, 10–12. doi: 10.14806/ej.17.1.200
- Martiny, A. C., Coleman, M. L., and Chisholm, S. W. (2006). Phosphate acquisition genes in *Prochlorococcus* ecotypes: evidence for genome-wide adaptation. *PNAS* 103, 12552–12557. doi: 10.1073/pnas.0601301103
- Martiny, A. C., Tai, A. P., Veneziano, D., Primeau, F., and Chisholm, S. W. (2009). Taxonomic resolution, ecotypes and the biogeography of *Prochlorococcus*. *Environ. Microbiol.* 11, 823–832. doi: 10.1111/j.1462-2920.2008.01803.x
- Mazard, S., Ostrowski, M., Partensky, F., and Scanlan, D. J. (2012). Multi-locus sequence analysis, taxonomic resolution and biogeography of marine *Synechococcus*. *Environ. Microbiol.* 14, 372–386. doi: 10.1111/j.1462-2920.2011.02514.x
- Ngugi, D. K., Antunes, A., Brune, A., and Stingl, U. (2012). Biogeography of pelagic bacterioplankton across an antagonistic temperature-salinity gradient in the Red Sea. *Mol. Ecol.* 21, 388–405. doi: 10.1111/j.1365-294X.2011.05378.x
- Parsons, T. R., Maita, Y., and Lalli, C. M. (1984). *A manual of chemical and biological methods for seawater analysis* (New York: Pergamon).

Publisher's note

All claims expressed in this article are solely those of the authors and do not necessarily represent those of their affiliated organizations, or those of the publisher, the editors and the reviewers. Any product that may be evaluated in this article, or claim that may be made by its manufacturer, is not guaranteed or endorsed by the publisher.

Supplementary material

The Supplementary Material for this article can be found online at: <https://www.frontiersin.org/articles/10.3389/fmars.2024.1456799/full#supplementary-material>

- Pedrós-Alió, C. (2012). The rare bacterial biosphere. *Annu. Rev. Mar. Sci.* 4, 449–466. doi: 10.1146/annurev-marine-120710-100948
- Penno, S., Lindell, D., and Post, A. F. (2006). Diversity of *Synechococcus* and *Prochlorococcus* populations determined from DNA sequences of the N-regulatory gene *ntcA*. *Environ. Microbiol.* 8, 1200–1212. doi: 10.1111/j.1462-2920.2006.01010.x
- Post, A. F., Penno, S., Zandbank, K., Paytan, A., Huse, S. M., and Welch, D. M. (2011). Long term seasonal dynamics of *Synechococcus* population structure in the Gulf of Aqaba, Northern Red Sea. *Front. Microbiol.* 2. doi: 10.3389/fmicb.2011.00131
- Rasul, N. M., Stewart, C., and Nawab, Z. A. (2015). “Introduction to the Red Sea: its origin, structure, and environment,” in *The Red Sea: the formation, morphology, oceanography and environment of a young ocean basin*. Eds. N. M. Rasul and I. C. Stewart (Heidelberg: Springer), 1–28.
- Righetti, D., Vogt, M., Gruber, N., Psomas, A., and Zimmermann, N. E. (2019). Global pattern of phytoplankton diversity driven by temperature and environmental variability. *Sci. Adv.* 5, eaau6253. doi: 10.1126/sciadv.aau6253
- Rognes, T., Flouri, T., Nichols, B., Quince, C., and Mahé, F. (2016). VSEARCH: a versatile open source tool for metagenomics. *PeerJ* 4, e2584. doi: 10.7717/peerj.2584
- Saito, M. A., Rocap, G., and Moffett, J. W. (2005). Production of cobalt binding ligands in a *Synechococcus* feature at the Costa Rica upwelling dome. *Limnol. Oceanogr.* 50, 279–290. doi: 10.4319/lo.2005.50.1.0279
- Scanlan, D. J., Ostrowski, M., Mazard, S., Dufresne, A., Garczarek, L., Hess, W. R., et al. (2009). Ecological genomics of marine picocyanobacteria. *Microbiol. Mol. Biol. Rev.* 73, 249–299. doi: 10.1128/MMBR.00035-08
- Schloss, P. D., Westcott, S. L., Ryabin, T., Hall, J. R., Hartmann, M., Hollister, E. B., et al. (2009). Introducing mothur: Open-source, platform-independent, community-supported software for describing and comparing microbial communities. *Appl. Environ. Microbiol.* 75, 7537–7541. doi: 10.1128/AEM.01541-09
- Shibl, A. A., Haroon, M. F., Ngugi, D. K., Thompson, L. R., and Stingl, U. (2016). Distribution of *Prochlorococcus* ecotypes in the Red Sea basin based on analyses of *rpoC1* sequences. *Front. Mar. Sci.* 3. doi: 10.3389/fmars.2016.00104
- Shibl, A. A., Thompson, L. R., Ngugi, D. K., and Stingl, U. (2014). Distribution and diversity of *Prochlorococcus* ecotypes in the Red Sea. *FEMS Microbiol. Lett.* 356, 118–126. doi: 10.1111/1574-6968.12490
- Spatharis, S., Tsirtsis, G., Danielidis, D. B., Do Chi, T., and Mouillot, D. (2007). Effects of pulsed nutrient inputs on phytoplankton assemblage structure and blooms in an enclosed coastal area. *Estuar. Coast. Shelf. Sci.* 73, 807–815. doi: 10.1016/j.ecss.2007.03.016
- Tamura, K., Dudley, J., Nei, M., and Kumar, S. (2007). MEGA4: Molecular Evolutionary Genetics Analysis (MEGA) software version 4.0. *Mol. Biol. Evol.* 24, 1596–1599. doi: 10.1093/molbev/msm092
- Thomas, M. K., Kremer, C. T., Klausmeier, C. A., and Litchman, E. (2012). A global pattern of thermal adaptation in marine phytoplankton. *Science* 338, 1085–1088. doi: 10.1126/science.1224836
- Tittensor, D. P., Mora, C., Jetz, W., Lotze, H. K., Ricard, D., Berghe, E. V., et al. (2010). Global patterns and predictors of marine biodiversity across taxa. *Nature* 466, 1098. doi: 10.1038/nature09329
- Toledo, G., and Palenik, B. (2003). A *Synechococcus* serotype is found preferentially in surface marine waters. *Limnol. Oceanogr.* 48, 1744–1755. doi: 10.4319/lo.2003.48.5.1744
- Uitz, J., Claustre, H., Gentili, B., and Stramski, D. (2010). Phytoplankton class-specific primary production in the world’s oceans: Seasonal and interannual variability from satellite observations. *Global Biogeochem. Cycles* 24, GB3016. doi: 10.1029/2009GB003680
- Veldhuis, M. J. W., and Kraay, G. W. (1993). Cell abundance and fluorescence of picoplankton in relation to growth irradiance and nitrogen availability in the Red Sea. *Neth. J. Sea. Res.* 31, 135–145. doi: 10.1016/0077-7579(93)90003-B
- Vergin, K. L., Done, B., Carlson, C. A., and Giovannoni, S. J. (2013). Spatiotemporal distributions of rare bacterioplankton populations indicate adaptive strategies in the oligotrophic ocean. *Aquat. Microb. Ecol.* 71, 1–13. doi: 10.3354/ame01661
- Weikert, H. (1987). “Plankton and the pelagic environment,” in *Key Environments-Red Sea. International Union for Conservation of Nature and Natural Resources. IV Series*. Eds. A. J. Edwards and S. M. Head (Oxford: Pergamon Press), 90–111.
- West, N. J., Schönhuber, W. A., Fuller, N. J., Amann, R. I., Rippka, R., Post, A. F., et al. (2001). Closely related *Prochlorococcus* genotypes show remarkably different depth distributions in two oceanic regions as revealed by *in situ* hybridization using 16S rRNA-targeted oligonucleotides. *Microbiology* 147, 1731–1744. doi: 10.1099/00221287-147-7-1731
- Xia, X., Cheung, S., Endo, H., Suzuki, K., and Liu, H. (2019). Latitudinal and vertical variation of *Synechococcus* assemblage composition along 170° W transect from the South Pacific to the Arctic Ocean. *Microb. Ecol.* 77, 333–342. doi: 10.1007/s00248-018-1308-8
- Xia, X., Guo, W., Tan, S., and Liu, H. (2017). *Synechococcus* assemblages across the salinity gradient in a salt wedge estuary. *Front. Microbiol.* 8. doi: 10.3389/fmicb.2017.01254
- Zhang, J., Kobert, K., Flouri, T., and Stamatakis, A. (2013). PEAR: a fast and accurate Illumina Paired-End reAd mergeR. *Bioinformatics* 30, 614–620. doi: 10.1093/bioinformatics/btt593
- Zwirgmaier, K., Jardillier, L., Ostrowski, M., Mazard, S., Garczarek, L., Vaulot, D., et al. (2008). Global phylogeography of marine *Synechococcus* and *Prochlorococcus* reveals a distinct partitioning of lineages among oceanic biomes. *Environ. Microbiol.* 10, 147–161. doi: 10.1111/j.1462-2920.2007.01440.x